Characterization of sorted stone circles and their relationship with vegetation in the Barton Peninsula in Antarctica using UAV data

Marta Melissa Canuto Almeida

marta_melissa@hotmail.com

Instituto Superior Técnico, Lisboa, setembro 2020

Abstract

The present work intends to provide a more detailed and spatially extensive characterization of the sorted stone circles. A large number of sorted stone circles (2927) obtained through images acquired via UAV (unmanned aerial vehicle or drone) were studied in one of the main regions of occurrence on the Barton peninsula on the island of King George (62ºS). The first part of this work goes through the outline of each of the circles, from which the parameters of size and shape (2D) and volume of the circle(3D) were extracted. In the second part, the images are classified using the SVM (Support Vector Machines) method, incorporating the Green Leaf Index (GLI) vegetation index in order to improve their performance and assess the relationship of the circles with the occurrence of vegetation. Through the analysis of the trends of the characterization parameters and the classification carried out, it was found that the circles at the less elevated areas have larger dimensions, diameters while at higher altitudes areas, the circles are smaller, with smaller volumes of stones and are covered with a higher percentage of vegetation (usnea). Generally speaking, the inner region of the circle did not show great variations with the increasing of the altitude.

Key words: Antarctica, patterned ground, sorted circles, usnea, UAV

1. Introduction

Surface patterns are formations commonly observed on soils in polar and high mountain periglacial regions, but also on other planetary surfaces in the Solar System, for example, on Mars.

These patterns can have different geometries, such as polygonal, lines or streaks, networks and circles, which may or may not be sorted according to the size distribution of the geological material that constitutes them (Washburn, 1956).

The typology of the patterns addressed in this work corresponds to sorted stone circles, which are metric circular shapes with a circular center essentially constituted by soil (*s.l.*) and surrounded by an over-elevated ring consisting of coarse rock sediments.

The formation of surface patterns is dynamic and polygenetic (Washburn, 1956). According to Kessler and Werner (2003), the type of pattern generated will depend on parameters such as the slope, the degree of confinement of the material, and the ratio between rock and soil.

The general model of formation of stone circles has been enriched over the last few years, but in some aspects, it is still open.

In 2001, Kessler *et al.* refers to 3 mechanisms, previously proposed by other authors, to introduce the development model of sorted stone circles: The first refers to the convective model of soils (Mortensen, 1932; Washburn, 1956; Hallet & Prestrud, 1986). The second mechanism addresses the frost heave mechanism at inclined freezing fronts that keep

the circles sorted through the upward movement of the rocky material and, consequently, a downward movement of the finer-grained particles (Nicholson, 1976). The third mechanism is also associated with the "frost heave" mechanism. But in this case, however, the downward movement results in the dissection and compaction of the soil, accompanied by vertical expansion during defrost, and internal transport of the soil along a defrosted and concave front to the surface.

The numerical model presented by Kessler *et al.* (2001) addresses the initiation, formation, and maintenance of sorted circles. In the conceptual model, sorted circles are generated in an active layer that is subjected to annual freeze-thaw cycles. The mechanisms that proceed in the active layer interact with the rocks and the soil in a different way due to the different physical and chemical properties of the lithologies. The resulting feedback promotes the emergence of sorted circles.

In contrast to the soil circulation model, in which the differential freezing front does not require soil saturation, this process does not require the existence of a permafrost zone or seasonal deep freezing and can occur only due to daytime surface freezing, despite the fact that both mechanisms can act simultaneously in the same place (Matsuoka *et al.*, 2003).

2. Image acquisition and case study

During February 2018, aerial surveys were carried out by a Portuguese team as part of a field campaign with logistical support from the Portuguese Polar Program (PROPOLAR) and the Korean Polar Institute (KOPRI) (Pina *et al.*, 2018).

The study areas covered in this work are located in Antarctica, in the South Shetland Islands, more precisely in the southwest of King George Island, on the Barton Peninsula (62º14'S, 58º46'W; WGS84). In this work, eight sites of the Barton peninsula were studied, ranging in altitude *a.s.l.* from 65 m to 250 m and that correspond to the main horizontal platforms of the Barton peninsula where the vast majority of sorted stone circles are located (López-Martinez *et al.*, 2012).

The acquisition and processing work results in the images used in this work in order to characterize the sorted stone circles and classify the obtained images.

3. Methodology

The present work is organized in two main parts, the first consisting on the characterization of the circles and the second in the classification of vegetation in the area of occurrence of the circles. At the end, any correlations are evaluated (Figure 1).

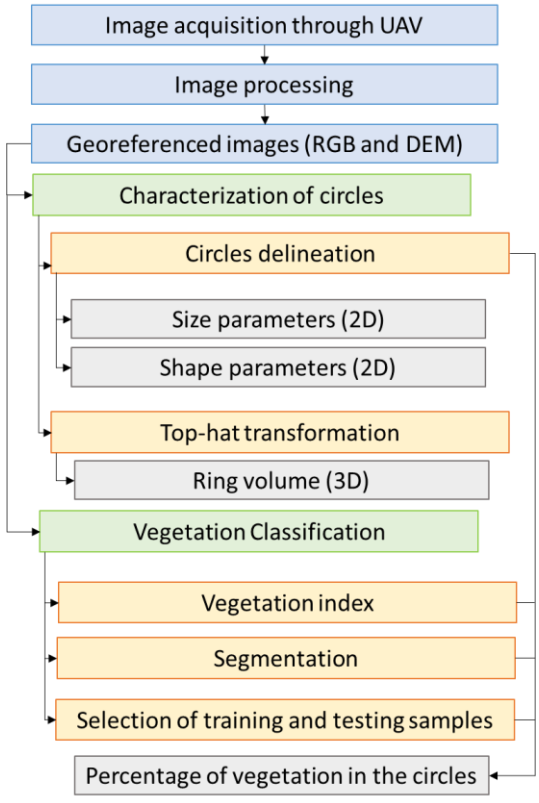

Figure 1- Simplified flowchart of the methodology.

3.1 Circles characterization

The identification of each region was carried out using the ArcMap 10.5 program, which consisted of creating polygons (in shapefile format) for each of these regions of the sorted stone circles. The parameters extracted in this work are organized into three groups:

- Size (2D) - area and perimeter of the different regions, the ratio between the interior and total area, thickness of the ring, the average diameter of the circles and diameter of the ring rocks.
- Shape (2D) - Major and minor axis, circularity, aspect ratio and density of circles.
- Volume (3D) - Volume of the ring region

The calculation of the ring volume was achieved through the application of the top-hat transformation (Meyer, 1979), which allowed extracting from a gray level image the peaks (white top-hat , wTH) in the DEM, corresponding to the clast ring.

This transformation corresponds to the difference between the initial image (*f*) and its opening ($\gamma^B(f)$), where B corresponds to the structuring element used in the opening. Two methodologies were developed in order to select the best size of the structuring element of the top hat for each site (Figure 2).

The first is performed in a quantitative manner, in which, once the tables for the various values of the top hat are obtained, the minimum volume values are identified: once the minimum equal to 0 is identified, the value of the previous top-hat will be chosen to calculate the volume of circles on that site.

The second methodology used corresponds to a visual choice in which, once the rasters of the various top-hat values are superimposed on the RGB images of each corresponding site, the value that best fits the reality of the circles is chosen.

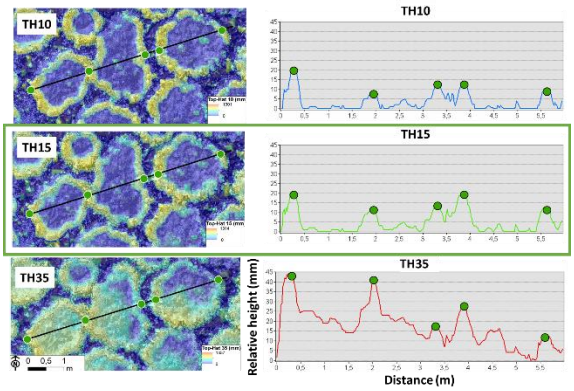

Figure 2- Example of the result of the application of the white top-hat transformation (Images on the left) Raster resulting from the application of the white top-hat with different values of the dimension of the structuring element (TH = 10,15 and 35) and (Images on the right) corresponding profiles, with TH = 15 being the chosen value.

3.2 Vegetation Classification

The classification of image mosaics was carried out using the ENVI 5.3 program, using automatic object-based methods (module "Feature extraction - Example Based"). To classify the various coverings existing in the fields of sorted circles, the following 5 classes were identified: rock, soil, lichens (usnea), moss and snow (if any).

It started by simplifying the images by reducing their spatial resolution (8x). The segmentation process, carried out at ENVI 5.3, is based on the Watershed transformation (Soille, 2004). The segmentation sequence in ENVI is accomplished by adjusting the parameters 'Scale Level' and 'Merge Level'.

In order to highlight the vegetation, different vegetation indexes in the literature were tested, based only on the components in the visible region of the electromagnetic spectrum, namely: Green leaf index (GLI); Modified green-red vegetation index (MGRVI); New green-red vegetation index (NGRVI); Red green-blue vegetation index (RGBVI); Visible

Atmospherically Resistant Index (VARI) and the Normalized Green Red Difference Index (NGRDI).

The effectiveness of the classifier was also tested through the use of DEM as Ancillary Data and the images resulting from the application of the "Topographic Modeling" tool that describe the geometric characteristics that represent the change in the surface.

For the classification of images, training and test samples were chosen. Once the classification is obtained, the results are compared to the reference set (ground-truth) to build the confusion matrix.

In this work, the validation of the results is based on the Overall accuracy ("OA") and the Kappa coefficient. The goal is to achieve results as close as possible to 100% or 1, respectively.

4. Results and discussion

4.1 Circles delineation

A total of 2927 stone circles were identified, arranged in the 8 identified sites (Table 1) and the outer and inner contours for each of the circles were delimited.

Table 1- Number of sorted circles identified by site.

Sites	Number of circles	Altitude (m)
01	88	67,4
02	85	84,3
03	169	117,5
04	107	138,5
05	937	180,2
06	615	88
07	706	182,7
08	220	245,9
Total	2927	-

Site 01 corresponds to one of the sites with the lowest number of observed circles, however, the circles do not have the most regular circular shape. There are also small areas of the study area that present snow / ice, a situation that also occurs on site 05. On site 02 there is an exceptionally different coloring of the terrain, more specifically of the soil that presents colors from ocher to reddish color.

Site 03 has noticeably smaller circles and it is interesting to highlight the existence of areas in which an apparent initial ordering of the rocks is observed, where small concentric depressions are visible, corresponding to less well defined circles and which are possibly (or were) in a less advanced state of evolution. Site 04 is relatively close to site 03, the circles are, however, noticeably more irregular and complex. The sorted circles of site 05 have an easily identifiable exterior contour, mainly due to the contrast between the mosses around the rocks of the circles. However, the contour of the inner circle is sometimes difficult as the soil-rock transition is not always well defined. At site 06 the circles are quite regular and, unlike site 05, the interior region is also quite well defined. The outer delimitation of the circles on site 07 is greatly facilitated by the contrast of colors with the intersection zone. Despite everything, the contour of the inner area of the circle is, in general, not as noticeable as that of site 06. Site 08 is in the highest altitude area studied on the Barton Peninsula. The circles are very close to each other, so there is little inter-circle space. This site also has a noticeably higher amount of vegetation (usnea) concentrated in the ring area.

4.2 Circle characterization

The delimitation of the circles allowed the extraction of information from the geometry of each analyzed circle.

Regarding almost all the 2D size parameters calculated (diameter of the circles, interior area, ring area, an outer perimeter, interior perimeter, thickness, and diameter of the ring rocks), the decrease is noticeable with increasing altitude.

There is a decrease in the area of the inner zone of the circle with increasing altitude, with average values ranging from 1,5 m^2 to 0,3 m^2. This variation interval is not so significant when compared to the ring area, which presents average values from 4,27 m^2 to 1,65 m^2 and even higher standard deviation values.

The average maximum thickness of the ring is shown in the graph in Figure 3.The variation of this parameter has a decreasing trend, from 0,52m to 0,28m, that is, in general, as the altitude increases, the maximum ring thickness decreases.

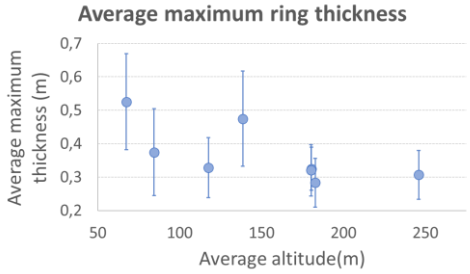

Figure 3- Scatter diagram of the maximum average ring thickness with the average altitude of each site and the respective vertical bars that represent the standard deviation.

As for the average diameter of the circles at the various sites, it is possible to see through the diagram of Figure 4, that there is a decrease in the same with the increase in altitude. The average diameter of the circles in the study zone it is 2,1m, which is relatively small comparing with the diameter of the Spitsbergen circles (3,0 to 4,0 m) (Kessler, 2001).

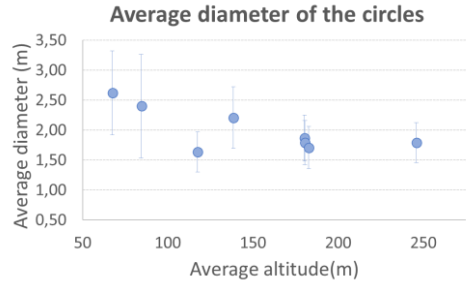

Figure 4- Scatter diagram of the average diameter of the circles and the respective vertical bars that represent the standard deviation.

The study carried out on the diameter of the ring rocks is merely illustrative, since the process involved was manual and with relatively few samples (30 measurements per site). Despite the number of samples, it is possible to observe a decreasing trend in diameter with increasing altitude, with range values going from 0,21 m to 0,08 m.

Regarding the shape parameters (2D), the mean values of the axes (major and minor) were considered and calculated; aspect ratio; circularity and the density of circles.

There is no significant trend in the aspect ratio variation, with the average values, in general, within the range of 0,75 and 0,79 and the standard deviation values being quite similar.

The circularity (Figure 5) , like the aspect ratio, does not show a significant variation of the values with the increase in altitude, these are within the range of values from 0,83 to 0,92.

The average circularity of the circles generally presents values very close to each other, apart from site 01 and site 02. Sites 01 and 02 show a slight variation in circularity with increasing altitude, and it should be noted that site 01 presents values standard deviation relatively higher than the others.

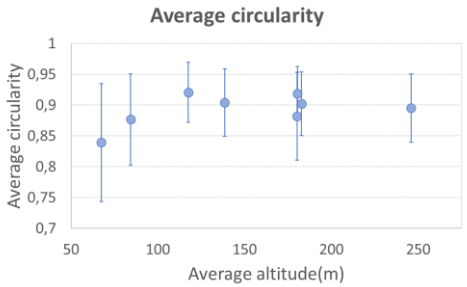

Figure 5 – Scatter diagram of the average circularity value with the average altitude and the respective vertical bars that represent the standard deviation.

An increase in the density of circles is observed from site 01 to site 08, with a minimum value of 0,04 circles/m^2 and maximum value of 0,25 circles / m^2.

The ring volume represents the 3D parameter covered in this document. To calculate the volume of the ring of the circles, obtained through the white top-hat transformation, several sizes for the structuring element were tested in order to select the appropriate value at each site. This assessment was carried out based on the visual method and the minimum value method greater than zero.

Depending on the method used, the volume values shown in the graphs Figure 6A and 6B, are obtained. In both methods, the volumes show a general decreasing trend, noting, however, that the method of minimums presents a more uniform decline when compared with the visual method.

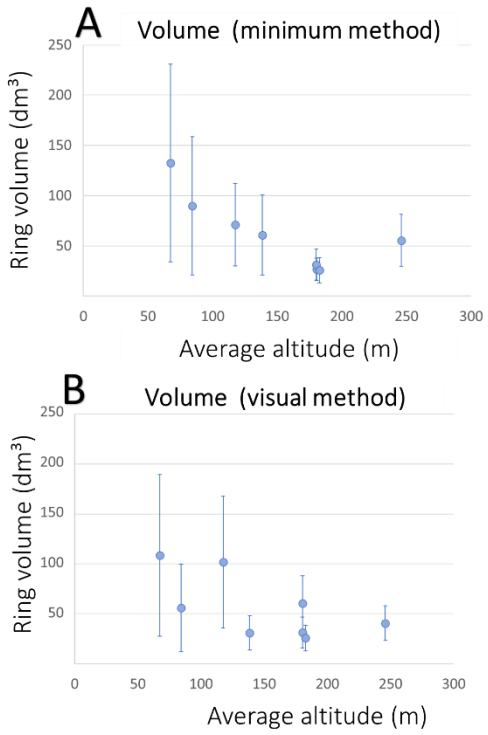

Figure 6 - Scatter diagrams of the average volume value of the ring zone and the respective vertical bars that represent the standard deviation.(A) Top-hat value used to calculate the volume, chosen using the minimum method. (B) Top-hat value used to calculate the volume, chosen through the visual method.

4.3 Vegetation Classification

Vegetation classification was performed using the ENVI 5.3 program, through the Feature extraction - Example Based tool. To this end, several segmentation and classification parameters were tested in order to obtain the best performance, also testing the inclusion of auxiliary variables such as the vegetation index based on RGB bands and the DEM.

Figure 7 shows the result of the calculation of the various vegetation indices. The GLI index was the one that showed the highest values of Overall Accuracy and Kappa and therefore corresponds to the index to be used in this work.

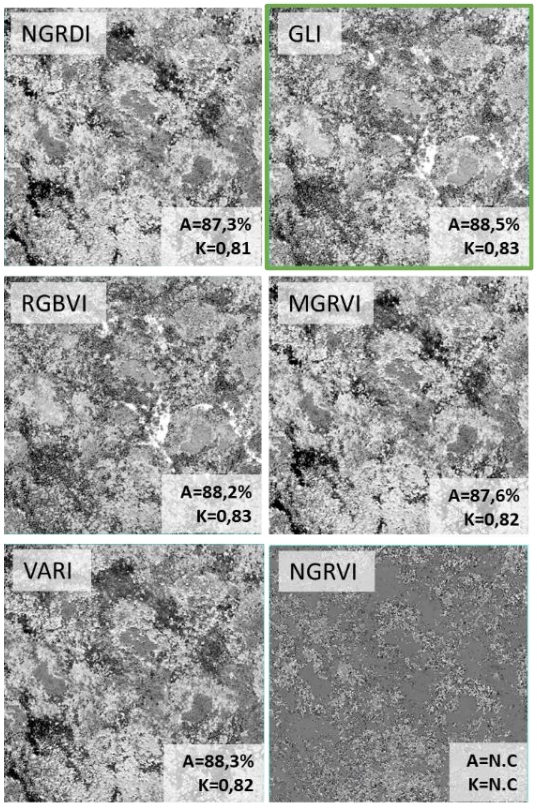

Figure 7 - Results of the calculation of the vegetation indices. The GLI index showing the best values for Overall Accuracy (OA) and Kappa (K). These indices have not been calculated (N.C) for the NGRVI index.

Then, the hypothesis that the DEM could be used to improve the previously obtained results was tested, however, it was found that, despite the similarity of results (Table 2), no

improvements were made in the classifier's performance.

Table 2-Results of the classification validation (Accuracy and Kappa values) using only the RGB image, the RGB set and the GLI vegetation index and finally, the RGB image with the GLI index and the digital terrain model (DEM).

	RGB	***RGB+GLI***	***RGB+GLI+DEM***
O.A (%)	91,10	91,79	90,60
Kappa	0,8602	0,8783	0,8605

To assess the importance of the relief, almost all the variables derived from the DEM were tested. The first test included the slope, aspect and parameters associated with convexities. In the second test, only the slope was used, and finally, in the third test, it uses only the data related to convexities as auxiliary data.

The results obtained in these 3 tests, and which are found in the Table 3, demonstrate that the use of the topographic parameters obtained through the DEM, does not increase the Overall Accuracy or the Kappa value previously obtained and exposed in Table 2. It appears that the use of the entire set of 8 geometric variables is clearly worse than the selective use of some of them.

Table 3-Results of the classification validation (Accuracy and Kappa values) using the images obtained through the topographic modeling tool. Almost all parameters are tested together, then only the slope and finally only the convexities.

	All the parameters	***Slope***	***Convexities***
O.A (%)	86,97	90,28	90,51
Kappa	0,8068	0,8564	0,8598

Considering the previously mentioned results, segmentation and final classification for each site is carried out, with the GLI vegetation index as an ancillary data. Summarizing, the segmentation parameters that best adapt to the images are between 20 and 30 for the Scale Level (S) parameter and between 50 and 70 for the Merge Level parameter (M) (Figure 8).

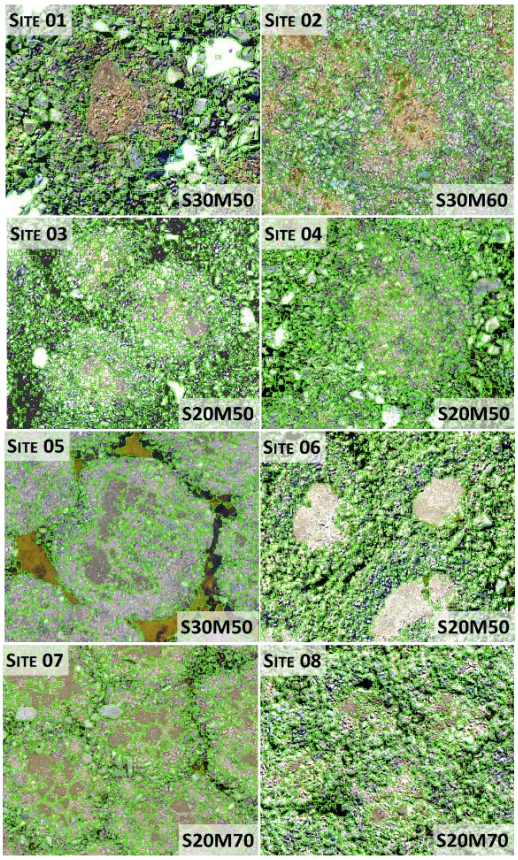

Figure 8- Results of the segmentation of the different sites (from 01 to 08) with the appropriate values of Scale Level (S) and Merge Level (M).

Once the images are segmented, the training and test samples are selected, and the classification is performed for each set of samples (Figure 9) . The overall accuracy values (A) are between 84,09% and 89,93% and the kappa values (K) between 0,71 and 0,87, and it can be said that the classifier generates a good performance in general.

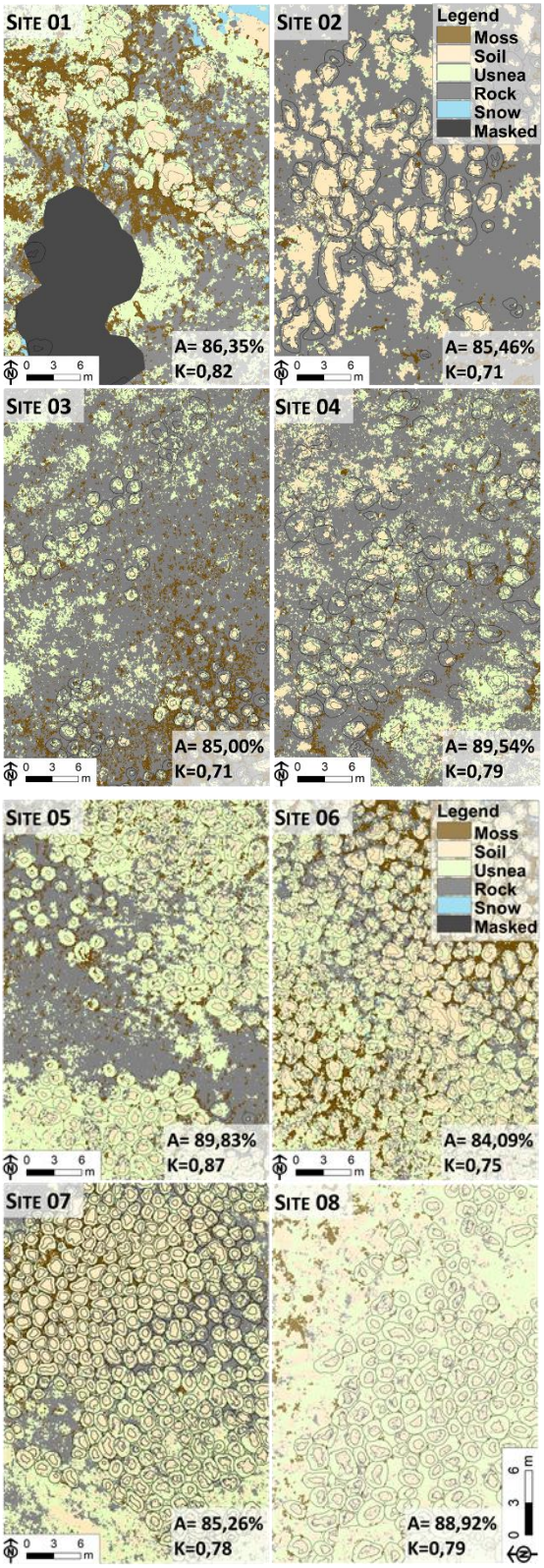

Figure 9 -Results of the classification of the sites from 01 to 08 with the 5 classes of study (moss, soil, usnea, rock and snow) and the zones with mask (Masked), with the respective value of overall accuracy (A) and kappa (K). The outlines of the circles correspond to the outlines made previously.

The analysis of the percentage variation of the classes shows that the variation of mosses is not significant with the increase of altitude, either in the inner zone of the circle or in the zone of the ring. In the inner area of the circle (Figure 10A) it is observed that, regardless of altitude, there is always a higher percentage of soil (ranging from 40% to 87%). This variation in the soil is approximately complementary to the variation in the percentage of usnea.

The results of the classification carried out in the ring area (Figure 10B) show that the percentage of exposed rock decreases (and the usnea increases) with altitude, reaching the highest value in site 08 (at an altitude of 245 m). This fact may, however, skew the calculation of the ring volume. For example, the positive variation of the ring volume from site 07 to site 08, may be associated with the amount of usnea observed in the ring at site 08, whose classification results have shown to be around 80% in the ring zone.

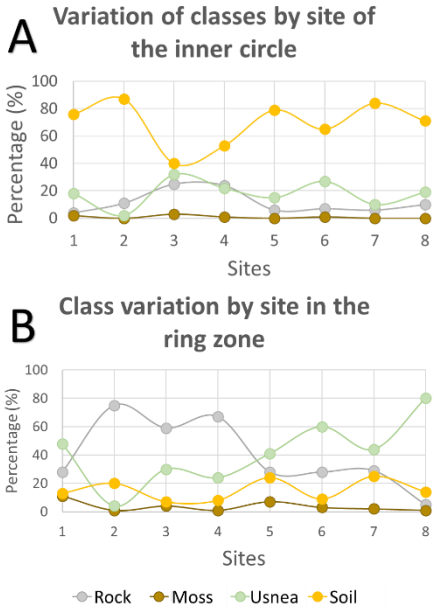

Figure 10- Average percentage variation of classes (rock, moss, usnea and soil) in the (A) inner zone of the circle and in (B) the circular ring for the various sites.

In short, in the areas of higher altitude, the circles, present less thick rings and a higher percentage of usnea. The growth of the area of

usnea is focused on the ring area since it is not observed inside the circle, therefore this relationship may be associated with sediment mobility. It can be assumed that the percentage of vegetation in the ring may be associated with the activity of the circular patterns, that is, the higher the percentage of vegetation in the ring, the greater the inactivity of the circle (Figure 11).

This deduction may be due to the fact that the usnea is not fixed in mobile sediments due to the associated dynamic process, which, according to the conceptual models referred to in chapter 1 , is inevitable in active circles, that is, during its formation and expansion.

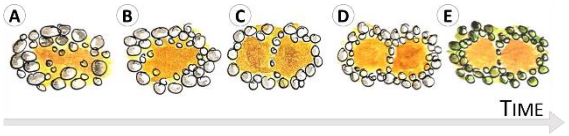

Figure 11-Simplified illustration of the temporal evolution of sorted stone circles. (A) Stone circle with poorly organized and relatively dispersed clasts. (B) Organization of clasts. (C) Subdivision of the sorted stone circle. (D) Sorted stone circles, after a long period of activity. (E) Sorted stone circles less active / inactive, with the fixation of vegetation (usnea) in the ring area. A to D illustration based on Kessler & Werner (2003).

The variation of parameters (such as the density of circles, thickness of the ring, and circularity, previously commented in this chapter), the gradation of the contrast between the different regions of the circles, but mainly the percentage increase of vegetation (usnea) with the increase of altitude, point to the possibility of circles located in higher altitude areas being less active or having had a shorter period of activity. The comparison with the only existing dating of these circles on the Barton peninsula (Jeong, 2006), aged between 290 and 4710 years obtained by radiocarbon in the analysis of vegetation debris buried in its central zone, was, however, not conclusive. It was not possible to detect any spatial age pattern in this study, perhaps because the dating was limited to a small number of circles (22 in total).

In conclusion, the observed results point to a possible hypothesis that the circles of the lower elevated zones are more active in certain periods due to a greater thickness of the active layer (Figure 12).

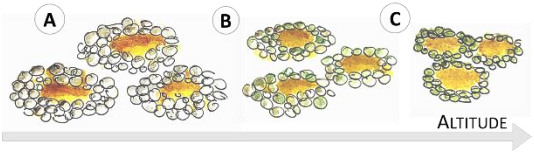

Figure 12- Simplified illustration of the variation of the sorted stone circles in the area of the Barton peninsula with the altitude. (A) Relatively low altitudes, spaced circles with comparatively high areas, thicknesses, perimeters and volumes. (B) Intermediate altitudes, increase in the percentage of usnea in the ring area, decrease in the area, perimeter and volume of the ring area. Increase in the density of circles. (C) Relatively high altitudes increase in the percentage of usnea and the density of circles. Comparatively smaller dimensions in terms of area, perimeter, decrease in the caliber of rocks and the volume of the ring zone. Little variation in the inner circle.

5. Conclusions

This work presents an advance relative to previous works, since through UAV data more extensive areas were studied and individually characterized a high number of patterns (total of 2927 circles), values that allow to obtain statistically more robust results when compared to the much smaller number of circles characterized in the field through more traditional approaches.

In general terms, the sorted stone circles analyzed on Barton peninsula on the island of King George have an average diameter of 2,1m and a circular ring 0,32m thick. Its average size clearly decreases in altitude (between 67m and 245m). Other size parameters were also calculated, as well as shape parameters and the volume of circular stone ring (using their own methods) and their relationship with altitude was evaluated.

The association of vegetation with stone circles was also approached in a pioneering way, through the automatic classification of the

various terrestrial surfaces. It was found that the existing vegetation in the ring zone (essentially usnea) tends to increase with increasing altitude, a relationship that has not been quantified in previous studies and is relevant information to be further investigated in future studies.

It is important to mention that, although the UAV data allow to obtain more and better information about the stone circles, its study and interpretation can still be improved with future studies. There are works that refer to the diversity of variables that can influence the geometry of sorted circles. The size of the circles may not be directly or solely associated with the depth of the active layer, the surface temperature must also be considered (Peterson, 2011).

Other factors must also be considered, such as the availability of sediment with different granularities, the lithological characterization of sediments and lateral confinement (Kessler & Werner, 2003). For future work it is, therefore, recommended to collect data in the field, at the study area, complementary to those of the UAVs. For example, sampling and characterizing soils at different depths and altitudes, characterizing the ring sediments, dating the circles, as well as monitoring the temperatures of the active layer. In addition, it is also advisable to incorporate in the acquisition of images by UAV a multispectral camera with sensors in the near infrared wavelength, as this way, it will be possible to improve the classification of vegetation.

Finally, the method for calculating the volume of circular ring introduced in this work requires improvement, mainly through a more sustained and detailed validation, since it proved to be very useful in calculating volumes.

6. References

Hallet, B., & Prestrud, S. (1986). Dynamics of periglacial sorted circles in western Spitsbergen. Quaternary Research, 26(1), 81-99.

Jeong, G. Y. (2006). Radiocarbon ages of sorted circles on King George Island, South Shetland Islands, West Antarctica. Antarctic Science, 18(2), 265-270.

Kessler, M. A., Murray, A. B., Werner, B. T., & Hallet, B. (2001). A model for sorted circles as self-organized patterns. Journal of Geophysical Research-All Series-, 106(7; Sect 2), 13-287.

Kessler, M. A., & Werner, B. T. (2003). Self-organization of sorted patterned ground. Science, 299(5605), 380-383.

López-Martínez, J., Serrano, E., Schmid, T., Mink, S., & Linés, C. (2012). Periglacial processes and landforms in the South Shetland Islands (northern Antarctic Peninsula region). Geomorphology, 155, 62-79.

Matsuoka, N., Abe, M., & Ijiri, M. (2003). Differential frost heave and sorted patterned ground: field measurements and a laboratory experiment. Geomorphology, 52(1-2), 73-85.

Meyer, F. (1979). Iterative image transformations for an automatic screening of cervical smears. Journal of Histochemistry & Cytochemistry, 27(1), 128-135.

Mortensen, H. (1932). Über die physikalische Möglichkeit der "Brodel"—Hypothese. Centralblatt für Mineralogie, Geologie und Paläontologie, 417-422.

Nicholson, F. H. (1976). Patterned ground formation and description as suggested by low arctic and subarctic examples. Arctic and Alpine Research, 8(4), 329-342.

Peterson, R. A. (2011). Assessing the role of differential frost heave in the origin of non-sorted circles. Quaternary Research, 75(2), 325-333.

Pina, P., Heleno, S., Vieira, G., Mora, C., Miranda, V., Hong, S.-G. (2018). Extensive mapping of sorted stone circles with ultra-high-resolution imagery: Preliminary results from the 2018 field campaign in Barton Peninsula, King George Island. Book of Abstracts of the 10th Portuguese Conference on Polar Sciences, 35, Universidade de Aveiro.

Soille, P. (2004). Morphological Image Analysis: Principles and Applications. Springer-Verlag, Berlin Heidelberg, 392 pp.